01 Feb 2023

Coreflooding Evaluation of Fiber-Assisted Recrosslinkable Preformed Particle Gel using an Open Fracture Model

Shuda Zhao

Ali Al Brahim

Junchen Liu

Baojun Bai
Missouri University of Science and Technology, baib@mst.edu

et. al. For a complete list of authors, see https://scholarsmine.mst.edu/geosci_geo_peteng_facwork/2103

Recommended Citation

S. Zhao et al., "Coreflooding Evaluation of Fiber-Assisted Recrosslinkable Preformed Particle Gel using an Open Fracture Model," *SPE Journal*, vol. 28, no. 1, pp. 268 - 278, Society of Petroleum Engineers (SPE), Feb 2023.
The definitive version is available at https://doi.org/10.2118/212282-PA

Coreflooding Evaluation of Fiber-Assisted Recrosslinkable Preformed Particle Gel Using an Open Fracture Model

Shuda Zhao[1], Ali Al Brahim[1], Junchen Liu[1], Baojun Bai[1]*, and Thomas Schuman[2]

[1]Department of Petroleum Engineering, Missouri University of Science and Technology
[2]Department of Chemistry, Missouri University of Science and Technology

Summary

Recrosslinkable preformed particle gels (RPPGs) have been used to treat the problem of void space conduits (VSC) and repair the "short-circuited" waterflood in Alaska's West Sak field. Field results showed a 23% increase in success rates over typical preformed particle gel (PPG) treatments. In this paper, we evaluated whether adding fiber into RPPGs can increase the RPPG plugging efficiency and thus further improve the success rate. We designed open fracture models to represent VSC and investigated the effect of swelling ratio (SR), fracture size, and fiber concentration on gel injection pressure, water breakthrough pressure, and permeability reduction. Results show that fiber can increase RPPG strength and delay its initial swelling rate, but an optimized fiber concentration exists. Beyond that, the fiber entangling problem can result in the recrosslinked bulk gel inhomogeneously and impact gel quality. The injection pressure of fiber-assisted RPPGs increased with the SR and fracture width. During post-injection water process, the breakthrough pressure and residual resistance factor increased when the RPPG SR and fracture width decreased. Fiber-assisted RPPGs can dramatically reduce the permeability of the fractured core up to 1.8×10^6 times. It is observed that the fiber-assisted RPPGs used in the experiment remain in a bulk form in the fracture when we open the fracture after water injection. Not only does the addition of fiber improve the plugging efficiency, but it also prevents particle precipitation along vertical fractures or conduits.

Introduction

Excess water production has become a major problem for oil fields, especially for mature reservoirs. Not only does it result in the quick decline of oil production rate, but it also results in an approximate cost of USD40 billion per year to dispose of the water in the world (Pu et al. 2019; Seright et al. 2001). Reservoir heterogeneity is one of the most significant reasons for the problem. Compared to a low-permeability zone, the pressure required for water flowing along a high-permeability zone (so-called thief zone) is relatively low, which leads more injected water to enter the high-permeability zone and create the channeling problem. Without a proper treatment, the channeling might result in a quick water production increase and eventually result in the well being abandoned despite a significant amount of oil remaining in unswept low-permeability zones or areas.

Gel treatment has been widely applied in oil fields to address the reservoir conformance and excessive water problems. In general, two types of gel systems have been used for the purpose, including in-situ gels and PPGs (Heidari et al. 2019). The in-situ gel system is composed of high-molecular-weight polymers and crosslinkers, and the mixture is injected into the target formation before they are crosslinked. Under reservoir temperature, the crosslinker will link the polymer chain to form a semisolid and immobile material (Amir et al. 2019; Bai et al. 2015; Heidari et al. 2019; Seright et al. 2001). As ConocoPhilips Co. first used in-situ gel in 1970, it has become the most common approach for conformance control due to its low cost, controllable gelation time, and easy operation. However, in-situ gel systems have distinct drawbacks, such as uncertainness of gelling due to shear from surface facilities and porous media, chromatographic problems during gelant transport through porous media when a large amount of gelant is injected, and potential damage in low-permeability zones due to gelant penetration into unswept zones or areas (Bai et al. 2007a). As an alternative, PPGs, which are manufactured in surface facilities, have been developed and applied in conformance control to overcome the distinct drawbacks inherent in the in-situ gelling system (Bai et al. 2007b). More than 10,000 field applications have proven the reliability of this technology, compared to many other available gel treatment technologies.

Numerous studies and field applications have demonstrated that both in-situ gels and PPG systems can be used to control preferential flow problems resulting from fracture and fracture-like features (Bai et al. 2015; Seright 1997). However, their field application results are often less than predicted in areas with large open fractures or conduits like the VSC in Alaska. RPPGs have been recently developed to improve the plugging performance of such abnormal features in mature oilfields (Pu et al. 2019). The RPPGs can swell after being placed into the brine, and the swollen particles can recrosslink with each other to form a bulky gel after a predetermined time by a pre-embedded crosslinking agent. Therefore, the gel maintains the advantages of both in-situ-crosslinking gels and conventional PPGs (Pu et al. 2019). The RPPG has been applied in the West Sak field in Alaska to treat the VSC and repair the "short-circuited" waterflood for more than 17 wells since April 2017. It was reported that 67% of the RPPG treatments held for more than 6 months compared to only 43% of the conventional PPG treatments (Targac et al. 2020). The successful application has proved that RPPGs can be a good gel candidate compared to cement, in-situ gel, foam gel, and PPG. However, there is still room available to further improve the success rate. Therefore, the method to combine fiber and RPPG has been proposed. It is expected that the combination can help to improve not only the RPPG plugging efficiency, but it can also prevent particles settling down in vertical fractures or conduits. Gel particles are denser than water, and they might settle down in the low part of a vertical fracture or conduit due to gravity before recrosslinking, which will result in an inadequate fracture filling. The subsequent injected water will concentrate in those vacant spaces, weakening the gel strength and increasing the pressure on the gels, which will increase the chances of their being broken down and washed out (Seright 2003).

*Corresponding author; email: baib@mst.edu

Original SPE manuscript received for review 15 December 2021. Revised manuscript received for review 1 August 2022. Paper (SPE 212282) peer approved 10 August 2022.

The purpose of this study is to evaluate whether fiber can be added into RPPGs to improve its plugging efficiency to vertical open fractures. A series of experiments have been conducted using our designed vertical fracture models and the effect of RPPG SR, fiber concentration, and fracture width on the breakthrough pressure, and the plugging efficiency effect is investigated. This work will provide conformance control engineers a better understanding of fiber-assisted RPPG behavior in open fractures, and assist them to design a more successful RPPG treatment.

Experimental Approach

Materials. ***RPPG.*** An RPPG sample from Daqing Xinwantong Technology Developing Co., Ltd. was used in this study. It is a crosslinked polyacrylamide and polyacrylic acid copolymer. The RPPG are small, white, solid particles with the particle sizes of 1 to 2 mm **(Fig. 1).** Its apparent density is about 1.39 g/cm^3. A dry RPPG particle can swell up to 40 times its volume after being placed in water and RPPG particles can recrosslink to form a bulk gel at reservoir conditions (Pu et al. 2019).

Fig. 1——(a) Dry RPPG particles. (b) Recrosslinked RPPG bulk gel. (c) Scanning electron microscope photograph of recrosslinked RPPG (Pu et al. 2019).

Brine. A 1% NaCl (10,000 ppm) solution was used for the RPPG swelling and coreflooding experiments.

Fiber. The fiber used in the study is a commercial product provided by Forta Co. The fiber is made of virgin homopolymer polypropylene with a length of 0.5 in. and an average width of 33 μm **(Fig. 2).** The specific gravity is 1.0.

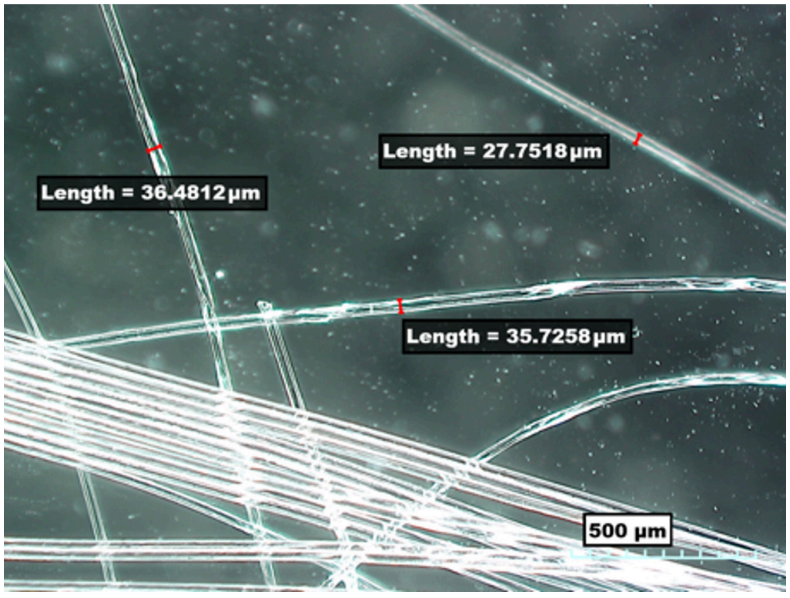

Fig. 2—Fiber from Forta Co. (average width = 33 μm, length = 0.5 in.). Image taken with Hirox-KH-8700 3D digital microscope (Hirox-USA Inc).

Fracture Model and Core Preparation. Cylindrical Berea sandstone cores (1.5 in. in diameter and 0.886 ft in length) were used to construct open fracture models. The cores were dried, evacuated, and saturated with 1% NaCl brine. To create the open fracture, each core was cut in half lengthwise and assembled again with two stainless steel strips supported. By adjusting the thickness of the steel strips, the fracture width can be controlled. The Reynolds number for different model parameters **(Table 1)** is between 0.3 and 3. To prevent possible leakage through the model, the core was wrapped with a thin PTFE tape. The created fracture was arranged vertically during the injection to reflect the practical fracture condition in reservoirs. **Fig. 3** demonstrates the open fracture model.

The fluid flow in the fracture between two smooth parallel plates can be expressed using the following equation (He et al. 2021):

Core No.	Fracture Width (mm)	Fiber (wt%)	Injection Rate (cm^3/min)	SR
1	1	0.1	0.5	17
2	1.77	0.1	0.5	17
3	2.33	0.1	0.5	17
4	2.7	0.1	0.5	17
5	1.77	0	2	17
6	1.77	0.1	2	17
7	1.77	0.3	2	17
8	1.77	0.1	5	6
9	1.77	0.1	5	11
10	1.77	0.1	5	17
11	1.77	0.1	5	20

Table 1—Coreflooding experimental design.

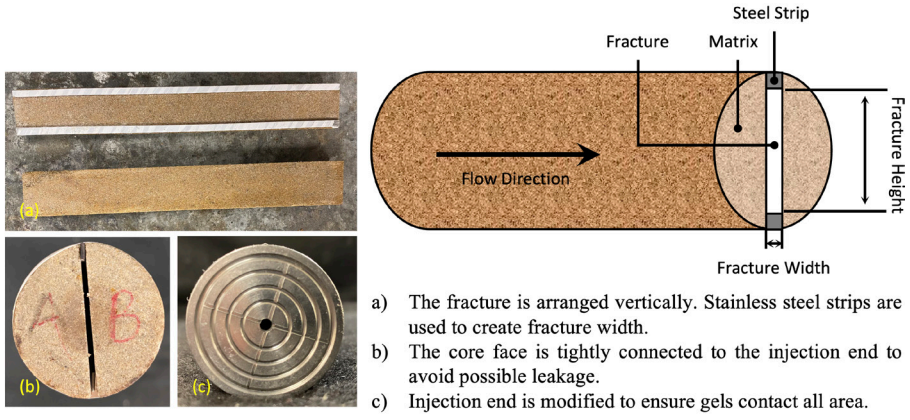

a) The fracture is arranged vertically. Stainless steel strips are used to create fracture width.
b) The core face is tightly connected to the injection end to avoid possible leakage.
c) Injection end is modified to ensure gels contact all area.

Fig. 3—Schematic of open fracture sandstone core.

$$Q = \frac{\Delta P h_f w_f^3}{12 \mu L}, \tag{1}$$

where Q is flow rate ; h_f is the fracture height; w_f is the fracture width; ΔP is injection pressure; L is the fracture length in the fluid flow direction; and μ is the fluid viscosity.

The overall permeability of the whole model, including both fracture and rock matrix, can be obtained by substituting the Darcy equation $Q = AK_t \Delta P/\mu L$ into Eq. 1 which gives:

$$K_t = \frac{h_f w_f^3}{12A}, \tag{2}$$

where K_t is the total permeability of the model and A is the cross-sectional area including both fracture and matrix.

Eleven cores were used in this study to evaluate the effect of fiber concentration, fracture width, and SR on injection pressure, water breakthrough pressure, and residual resistance factor. **Table 1** shows the experimental design. Four cores were used to evaluate the fracture width effect. Three cores were used to evaluate the fiber concentration effect. Another four cores were used to evaluate the SR effect.

Experimental Procedure. ***Fiber-Assisted RPPG Preparation.*** Because RPPG particles can recrosslink into a bulk gel after gelation, fibers can be added directly during the particle swelling process instead of the synthesis process. After recrosslinking, the fibers are incorporated into the bulk gel system which could further enhance the gel strength. The SR influences the bulk gel strength directly (Pu et al. 2019). By adjusting the amount of feeding brine, the final SR can be controlled. The preparation stages can be divided into four steps:

1. Spread fibers in the brine evenly.
2. Add RPPG particles into fiber dispersion.
3. Keep stirring the mixture to prevent gel particles from settle to the bottom.
4. Stop stirring until gel particles reach the maximum swelling in given volume of brine.

The SR is defined as:

$$SR = \frac{W_{\text{feeding brine}} + W_{\text{RPPG particles}}}{W_{\text{RPPG particles}}},$$

where $W_{\text{RPPG particles}}$ is the weight of dry RPPG particles and $W_{\text{feeding brine}}$ is the weight of feeding brine.

Swelling Kinetic and Stage Transition Test. Swelling kinetic is an important property for RPPG treatment design. According to the field study conducted by Targac et al. (2020), RPPG swelling kinetics can be divided into five transition stages **(Fig. 4):**

A. Initial slurry: free water visible at the top
B. Fully swollen: minimal free water remaining in the system; irregular surface observed
C. Tacky condition: stable in inverted position; grain boundaries still visible
D. Competent bond: grain boundaries still observed, but will suspend from hook
E. Fully bonded: fully bonded; granular contacts no longer visible.

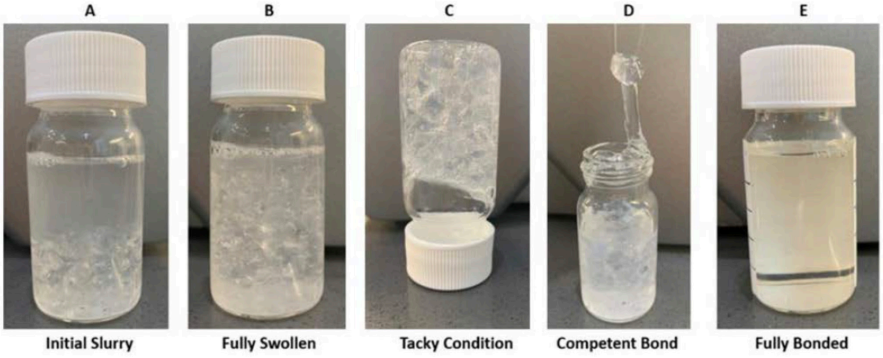

Fig. 4—Different stages of RPPG (Targac et al. 2020).

In our experiments, we used the same transition stages to evaluate the fiber-assisted RPPG system. The effect of fiber concentration on the swelling kinetic (Stages A to B) and stages transition (Stages B to E) was investigated **(Table 2).** F0 is the control sample without fiber. The swelling kinetic was evaluated at room temperature. During this process, samples were swollen under dynamic motion to avoid particle settling. The volume of the samples was recorded every 5 minutes. When Stage B was observed, samples were transferred to a 45°C oven for further observation. During this process, the condition of the sample was checked every 30 minutes. The time when each stage occurs was recorded.

Sample No.	Fiber (wt%)
F0 (control sample)	0.0
F1	0.1
F2	0.2
F3	0.3

Table 2—Fiber products and concentrations of each sample.

Rheology Test. After fiber-assisted RPPGs were fully recrosslinked, rheology tests were conducted to give a strength comparison between different fiber concentration samples. The RPPG samples used in these tests were prepared with 1% NaCl solution with an SR of 1:10. The HAAKE Mars Rheometer III was used to measure the G' (elastic modulus) and G'' (viscous modulus). Plate P35 Ti L S was used as the spin. The gap was 1 mm; the frequency was 1 Hz; τ was 10 Pa; and the duration was 300 seconds. The excess gel outside of the spin was carefully removed to avoid any possible disruption. Each sample was tested three times to get an average value.

Coreflooding Test. *Gel Injection.* In the gel injection process, the prepared fiber-assisted RPPG was injected into the open fracture under a constant flow rate. Before the injection, the core was wrapped with a thin PTFE tape to prevent the possible gel leakage through the gap between the fracture and steel strips. In the preparation process, Stage B is required to determine whether the gel is ready to be injected. If the gel particles are injected between Stages A and B, a large amount of free water is lost, which affects the fixed SR. Stages C, D, and E will take place inside the open fractured model. The injection process is finished when the pressure recorded at the core holder inlet is stable. It was found that injecting one fracture pore volume gel is not enough to fully fill the fracture because of the swelled gel dehydration while transporting through the fracture. Therefore, the stable injection pressure is an eligible condition to determine whether the fracture volume is fully filled with the gel particles and when to stop the injection. After injection, the core holder was shut in at 45°C to make sure the RPPG fully recrosslinked (Stage E). The shut-in time is designed based on the results of the stage transition test. The RPPG samples from effluent and accumulator (remained) were also collected and placed in the 45°C oven to be monitored to further ensure that the RPPG in the fracture is fully recrosslinked.

Fig. 5 is the coreflooding apparatus setup, which is mainly composed of one syringe pump, two accumulators, and one core holder. The core holder is heated to 45°C during the whole process and the confining pressure is always 500 psi higher than the injection pressure. The accuracy of the pressure sensor is $< \pm 0.75\%$ of full range. The outlet of the core holder was specially modified with three outlets, two of which are from the matrix and one from the fracture. Effluents from fracture and matrix can be collected from each independent outlet to provide more information about water diversion and matrix damage. The pressure gradient of gel injection, water breakthrough, and post-waterflooding is calculated by the injection pressure divided by the length of the fracture.

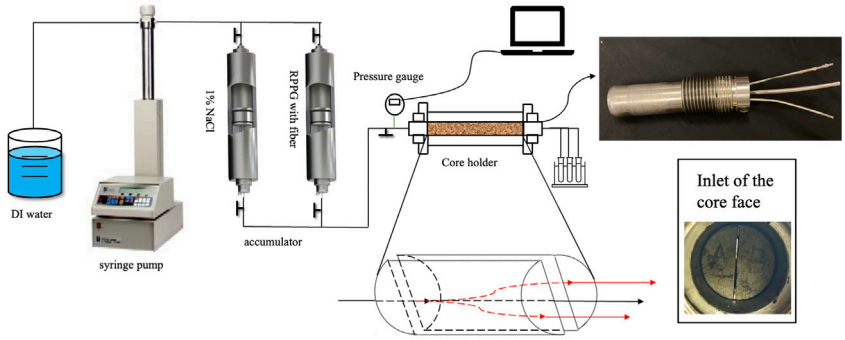

Fig. 5—Apparatus setup for RPPG with fiber coreflooding experiments.

Breakthrough Pressure Test. Breakthrough test is conducted to evaluate how much pressure the fiber-assisted RPPG can hold after recrosslinking inside the fracture. We used the constant pressure method to determine the breakthrough pressure. During the experiment, brine is first injected to the core at a constant pressure started at 20 psi and outlet is observed to see whether effluent comes out of the fracture. If no effluent come out in 3 minutes, the injection pressure is increased 5 psi for another 3 minutes, and this process continues until any effluent is produced from the fracture outlet. It is noted that the injection pressure when effluent starts to produce from the matrix outlet is not considered as the breakthrough pressure because our purpose is to evaluate the RPPG's blocking performance within the open fracture.

Post-Waterflooding Test. The post-waterflooding test is conducted to obtain the pressure response at different flow rates and to calculate the residual resistance factor (F_{rr}) which is the ratio of k_{before} and k_{after}. Four flow rates (0.25, 0.5, 0.75, and 1 cm^3/min) are applied to obtain the stable pressures, and each flow rate is run over 4 hours to make sure a steady state is reached.

Results and Analysis

Swelling Kinetic and Gel Stages Transition. The swelling kinetic of different samples are shown in **Fig. 6.** Based on the trend of gel volume change, the swelling rate of the gel varies significantly with time—rapid swelling and slow swelling. Taking F3 (Fiber: 0.3 wt%) as an example, the gel volume increased rapidly from 2 (initial dry particles volume) to 17 cm^3 in 5 minutes. This is because RPPG contains a large amount of hydrophilic functional groups, and it can absorb several times its volume of feeding water (Wang et al. 2019b). Then, the swelling speed slowed down and gel volume was increased by 3 cm^3 in 20 minutes. This is mainly caused by the presence of crosslinking structure in RPPG, which has a limitation of crosslinker density and grid size. In the slow swelling process, the osmotic pressure inside and outside the gel particle grid approaches the equilibrium, so that the subsequent water absorption rate tends to be stable. The similar phenomenon is also found in PPG and its derived gel system (Bai and Sun 2020; Zhao et al. 2021). The results showed that adding the fiber can accelerate the swelling process but it has no effect on the time to reach Stage B (fully swollen). Because the fiber density is close to water, floating fibers can hold some RPPG particles, which allowed the RPPG particles to have a larger water contact area and facilitated water absorption. This phenomenon can also reduce the particle settlement in a vertical fracture. However, such

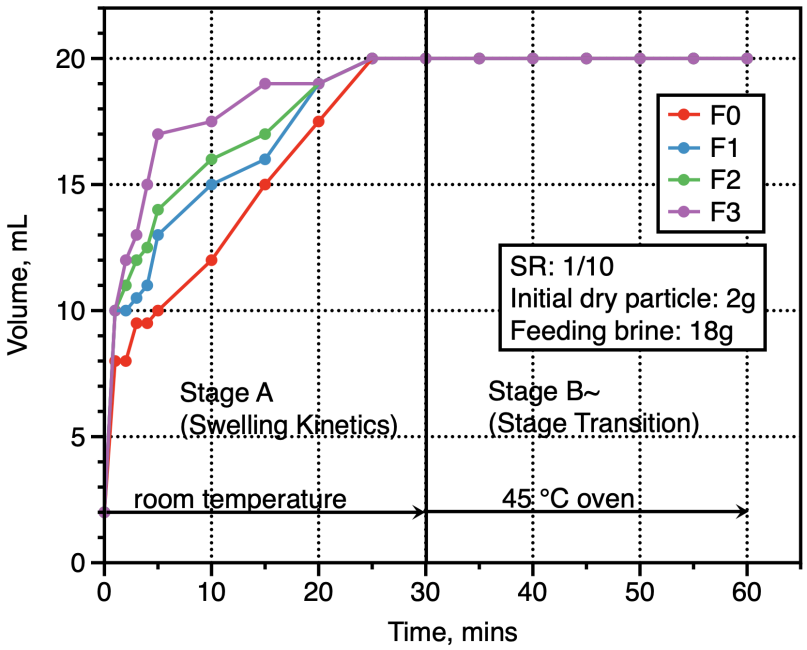

Fig. 6—Fiber concentration effect on swelling kinetic and stage transition.

swelling acceleration occurs only in the early stage. When particles can support themselves, Stage B still depends on the swollen RPPG itself rather than the fiber.

For subsequent stage transitions, samples were placed in an oven and their states were checked every 30 minutes. Results indicate that adding fiber delays the time required to reach Stages C and D but has no effect on Stage E. However, varying fiber concentrations do not influence the transitions. **Table 3** compares the times to reach different transition stages of fiber-free RPPG and fiber-assisted RPPG. Fiber-assisted RPPG takes 35 minutes to reach Stage C and 90 minutes to reach Stage D under 45°C. It is 5 minutes longer to reach Stage C and 15 minutes longer to reach Stage D compared with the control sample (zero fiber added). Both fiber-assisted RPPG and control samples can reach Stage D (fully recrosslinked) after 48 hours. The delay time is attributed to the physical impediment of particles contacting one another caused by the presence of fiber. Because of the volume limitation, the RPPG particles can eventually contact each other after the minimal free water is absorbed. As a result, the fiber does not affect the time required to reach the final stage.

Stages	Time	Time (Zero Fiber)
B	25 minutes	25 minutes
C	35 minutes	30 minutes
D	90 minutes	75 minutes
E	48 hours	48 hours

Table 3—Fiber effect on gel stage transition time.

The five stages are very important for a practical field application design (Targac et al. 2020). It is expected that Stage B can be reached when the gel starts to enter the fracture or VSC. If the RPPG enters the VSC or fracture before reaching Stage B, a large amount of free water will be lost and leave free water in the upper part of a vertical fracture. Ideally, the injected gel particles should remain between Stages B and C until they reach the target area. Stage C is when the gel particle interfaces start to disappear and gel strength starts to build up. Meanwhile, the gel particles also lose some mobilities at this stage, which makes it become immobile inside of the VSC compared to Stage B. The gel strength is further improved in Stage D. A stationary condition is helpful to develop bond connection efficiently. Stage E is the complete stage, where all the gel particle interfaces disappear, and the gel strength reaches its maximum.

Rheology. Fig. 7 illustrates the influence of fiber concentration on gel strength. The results indicate a considerable improvement on the gel strength when the fiber is introduced. When fiber is used as an additive, it is prepared with the feeding water so that it can be assimilated into the bulk gel system autonomously after the gel particles recrosslink. The gel strength increased until it reached the highest value of 839 Pa at 0.2 wt% fiber concentration, which is 21% improvement compared with the control sample (692.3 Pa). However, when the fiber concentration was increased to 0.3 wt%, the gel strength declined. A probable explanation is that a high fiber concentration can result in entanglement of fiber during the preparation process, which makes the recrosslinked bulk gel nonhomogeneous. In other words, certain areas of the gel have an excessive amount of fiber while others contain an insufficient amount. This issue also leads to a low water breakthrough pressure, which can be found in the next section. **Fig. 8** illustrates the entanglement of the fibers. When the fiber is

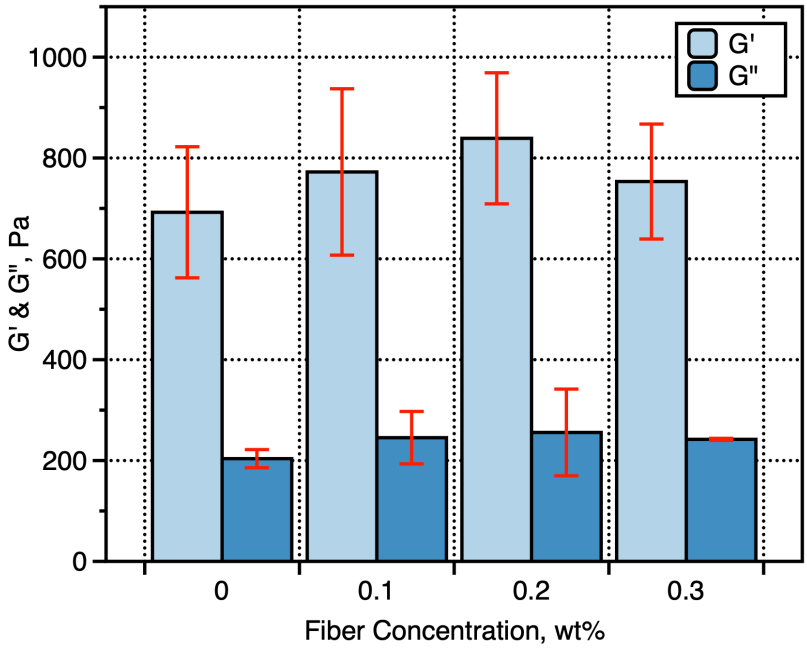

Fig. 7—Fiber concentration effect on gel strength.

prepared with the feeding water, entanglement begins to form. When gel particles are introduced and swelled, the entanglement of this fiber segment becomes more severe.

Fiber Concentration Effect. Fig. 9 shows the fiber concentration effect on injection. The injection process can be divided into two stages—pressure buildup and steady statewhich are the same as regular RPPG and PPG injection process (Pu et al. 2019; Wang et al. 2019a). Taking 0 wt% fiber concentration as an example, during the first 20 minutes of injection, the pressure gradient slowly built up to 6 psi/ft, and only fluid was produced at the fracture outlet, as shown in **Fig. 8a**. Then, the injection pressure increased rapidly, and particles were observed at the fracture outlet. After around 80 minutes, the pressure gradient was stabilized at around 62 psi/ft and all fluid disappeared and only gel particles were produced from the fracture outlet **(Fig. 10b).** This phenomenon indicates that when RPPGs transport in the fracture model, the front-end may contain more water than the back-end. One possible reason is that the pressure drop along the fracture causes the dehydration of the swollen gel particles. Seright found a similar phenomenon when he investigated preformed bulk gel transport through fractures (Seright 1999). The abrupt peak is likely caused by some large particles trapped by the fracture. RPPG without adding fiber shows faster pressure buildup and lower stable pressure. Based on the test in the previous section**,** gel stages transition was faster when no fiber was added, which caused pressure to build up fast. When the gel particles completely passed through the fracture and the pressure was stabilized, a higher stable pressure (75 ~ 80 psi/ft) was observed for RPPG with fiber because adding fiber can effectively increase the gel strength. However, there was no obvious pressure change for fiber concentrations of 0.1 and 0.3 wt%. Both experiments show that RPPG can pass through the fracture of which size is smaller than the particle size, indicating that adding fiber does not have a significant negative effect on particle deformability.

Although the outlet was modified and water was detected from all three outlets **(Fig. 10b)**, the data are not sufficient to indicate that RPPG particles may penetrate the rock matrix. The water produced from the matrix outlet may come from the initial water in the fracture or the water from gel dehydration. Additionally, no gel particles were produced from matrix outlets.

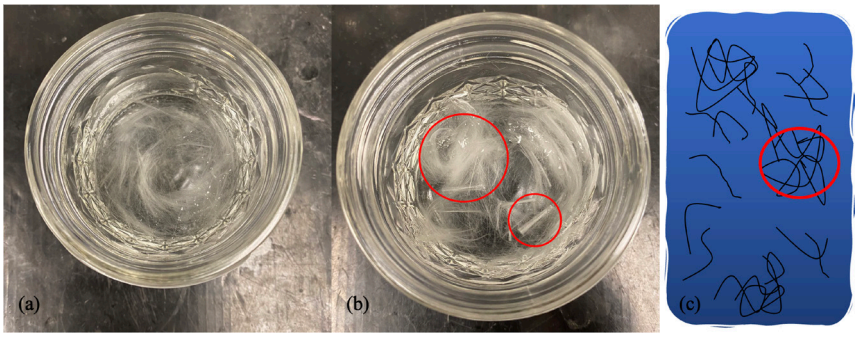

Fig. 8——(a) Low fiber content: homogeneous. (b) High fiber content: entanglement when prepared with feeding water. (c) Schematic of entangled fibers in bulk gel.

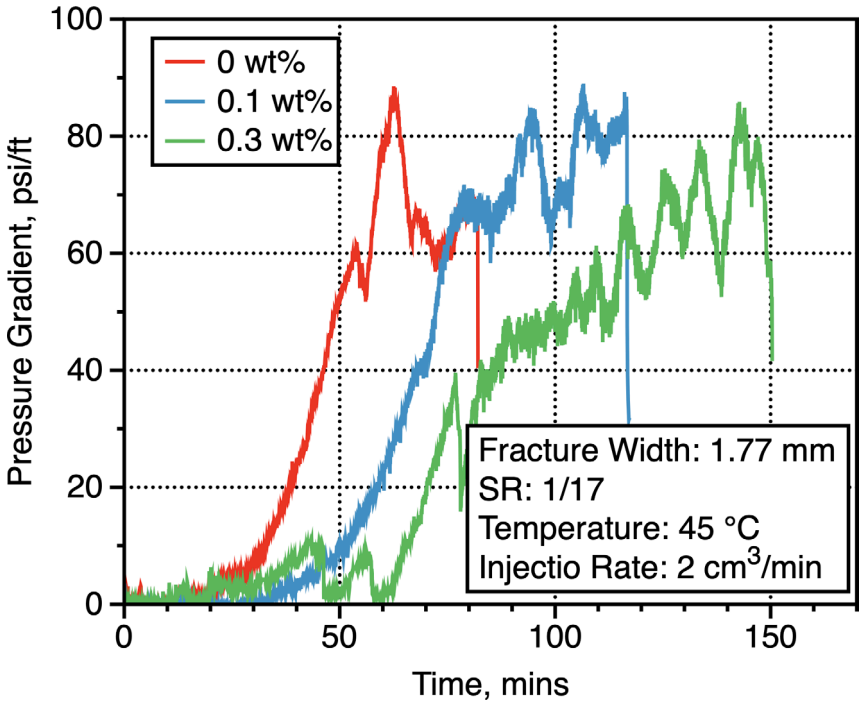

Fig. 9—Fiber concentration effect on gel injection.

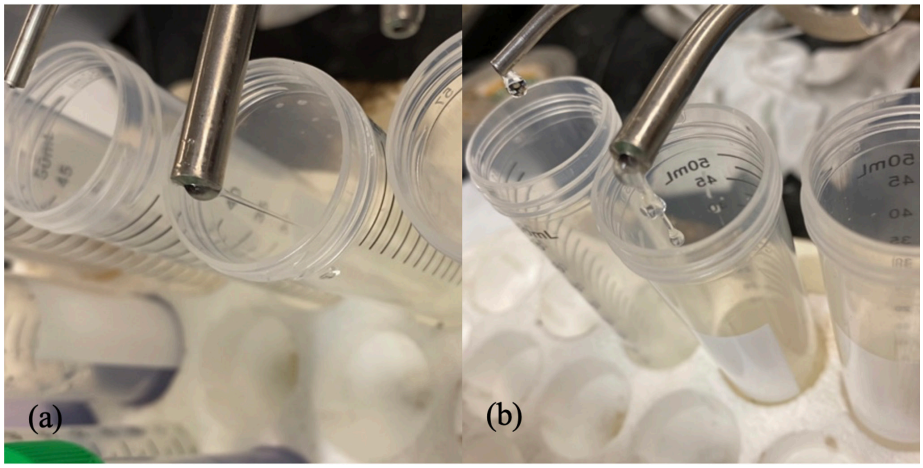

Fig. 10—Viscous polymer produced (a). Gel particles produced (b).

The water breakthrough pressure is depicted in **Fig. 11.** The sudden pressure drop at the end of each step indicates that RPPGs could no longer hold the pressure and water broke through the gel-treated core. The results indicate that adding 0.1 wt% fiber can increase the breakthrough pressure by 60% (52 psi/ft). When the constant pressure was loaded on the 0.1 wt% fiber-assisted RPPG-treated core, water was produced from the matrix outlet rapidly, as indicated by the uneven pressure step in **Fig. 11a**. Additionally, this phenomenon indicates that fiber addition might be more beneficial for water diversion. However, as fiber content increased to 0.3 wt%, the water breakthrough pressure decreased (~40 psi/ft). This finding is consistent with the results of the rheological testing: The entanglement of fibers resulted in a heterogeneous bulk gel. Constant loading pressure initially broke a small area, which contained less fiber, and then created a channel when the pressure was increased further **(Fig. 12).** Although the 0.1 wt% fiber-assisted RPPG sample contains less fiber, the homogenous structure has a superior pressure resistance performance.

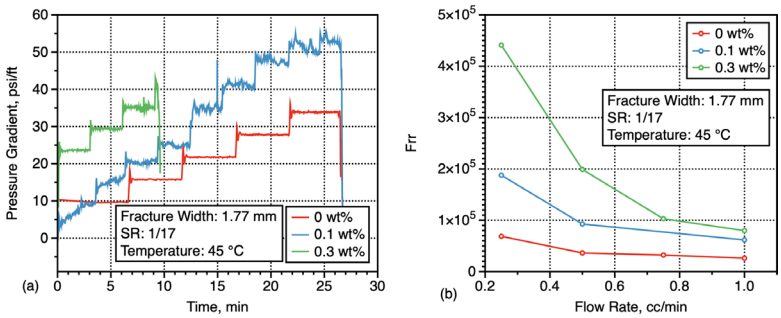

Fig. 11—Water channel created through weak parts.

Fig. 12—Fiber concentration effect on water breakthrough (a) and F_{rr} (b).

Fig. 11b shows the fiber concentration effect on F_{rr}. It should be noted that the F_{rr} improvement is significant when the flow rate is low, which indicates fiber-assisted RPPG has better water resistance in far wellbore locations. Although the breakthrough pressure for the 0.3-wt% fiber content sample is lower than 0.1 wt%, it shows a positive effect on F_{rr} for a long time waterflooding. It is related to how much gel can be retained in the fracture. When the water channel was constructed in the weaker region, the fiber-rich portion retained its original location to withstand water flushing. As a result, when the water channel is formed, the gel with a high fiber content has a greater advantage in terms of plugging efficiency.

According to a field application, 67% of the RPPG-treated wells held for more than 6 months compared to only 43% of the PPG treatments on a per treatment basis (Targac et al. 2020). The results in this study indicate that adding fiber could significantly improve the water breakthrough pressure as well as the residual resistance factor. Therefore, the use of fiber as an additive can help to improve the success rate. However, it should be noted that the plugging performance may not go straight up with increasing fiber concentration. Based on the rheology and water breakthrough test, there is an optimized fiber concentration because higher fiber concentration could cause an entanglement problem when mixed with RPPGs. As the entanglement problem is related to the fiber properties and dimension, such optimized concentration may vary among different fiber products

SR Effect. Fig. 13 illustrates the influence of the SR on injection pressure. There are two stages to the injection pressure gradient: pressure buildup and steady state. The results indicate that the lower the SR, the more rapidly the pressure gradient builds up. Because the gel particles are compressed and deformed as they move through the fractures, a stronger gel leads to a higher injection resistance. A higher SR resulted in a looser gel structure, which weakened and increased the fluidity of gels. Additionally, because of the vertical open fracture and gravity, RPPGs with higher SR tend to accumulate at the bottom. Therefore, it took longer for the high SR RPPG to completely fill the fracture and delayed the steady state.

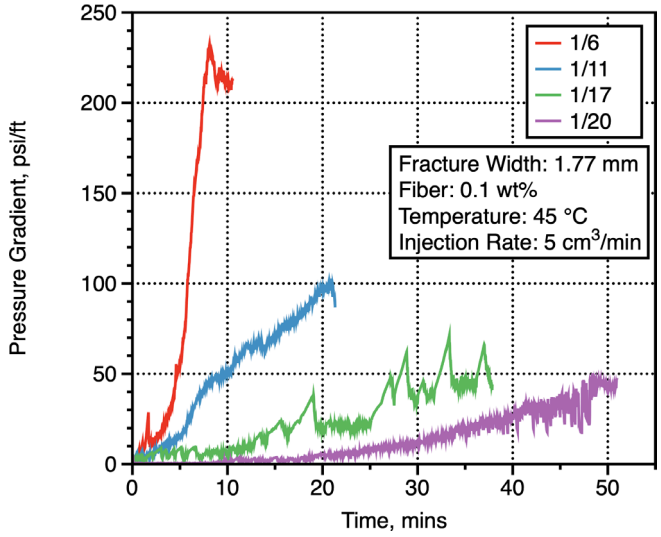

Fig. 13—SR effect on gel injection.

Fig. 14 shows the SR effect on water breakthrough and F_{rr}. **Fig. 14a** is the step pressure vs. time. The pressure drop at the end means water breaks through the fracture. The results show the SR of 1:6 has the highest breakthrough pressure gradient: 148 psi/ft, then the breakthrough pressure gradient decreases orderly as the SR increases. As mentioned above, a lower SR means a tighter gel structure, which makes the gel stronger and able to withstand higher pressure. **Fig. 14b** shows the SR effect on F_{rr}. As observed, F_{rr} increased with the decreased SR. As less feeding brine is absorbed in the gel structure, the pore structure of the low swelling RPPG is much tighter and therefore the gel is much stronger. Such tight gel structure provides a better strength and significant pressure resistance for the post-injection water.

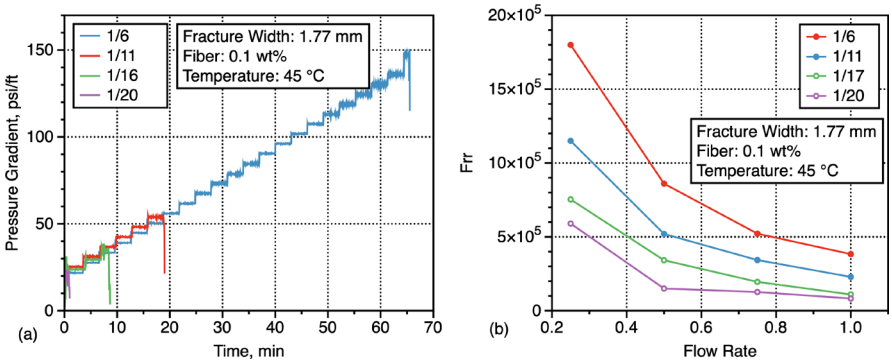

Fig. 14—SR effect on water breakthrough pressure (a) and F_{rr} (b).

SR directly affects the RPPG strength (Pu et al. 2019) and there is no doubt that it affects the RPPG injection pressure and plugging performance. Many results have been reported about the effect of salinity on SR, but few of them show how the SR affects the injection pressure and plugging performance. Oil companies can control the SR by adjusting the amount of feeding brine. Low SR gel has the advantages of high breakthrough pressure gradient and F_{rr}, but it results in higher injection pressure.

Fracture Width Effect. Fig. 15 shows the fracture width effect on gel injection. The gel injection can be divided into two stages: pressure buildup and steady state (stable injection pressure). It can be seen that stable injection pressure gradient increased with the decrease of

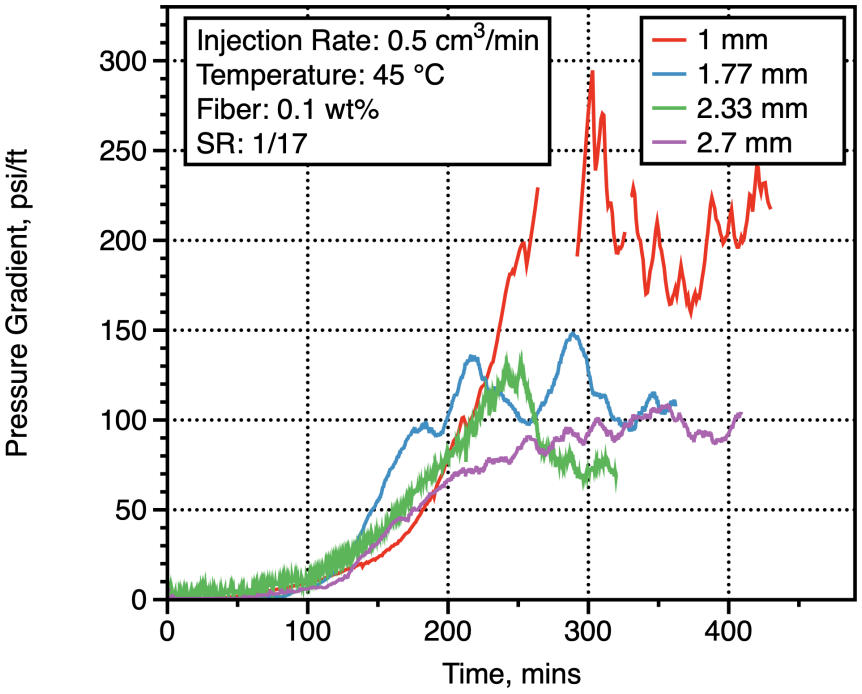

Fig. 15—Fracture width effect on gel injection.

fracture width, which is consistent with conventional PPG injection into a fracture (Zhang and Bai 2011). This is because when the gel particles are injected into a fracture smaller than their sizes, they deform and dehydrate to transport through the fracture, requiring a higher pressure drop to compensate for the deformation.

Fig. 16a shows the fracture width effect on water breakthrough. It can be seen that the narrow fracture width resulted in higher breakthrough pressure. When the fracture width was down to 1 mm, the breakthrough pressure increased significantly. This is because the gel received stronger compression in the narrower fracture during the injection. When the injection was finished, a tighter gel structure was passively created. Therefore, even though the gel had the same SR before the injection, the gel strength changed after the injection was completed. It is noted that the water pressure of the 1 mm fracture experiment did not drop dramatically like others after the breakthrough. Instead, the pressure became unstable and only matrix outlets were producing water, indicating water did not breakthrough the gel inside the fracture so the actual breakthrough pressure could be higher. **Fig. 16b** shows the fracture width effect on residual resistance factor F_{rr}. As observed, F_{rr} decreased with the increased fracture width, which means the gel successfully decreased the permeability of the gel-treated fracture and the effectiveness was affected by the fracture width. Consistent with the principle mentioned above, the gel particles received more extrusion and dehydrated more in a narrow fracture. Therefore, the F_{rr} for narrow fracture was higher.

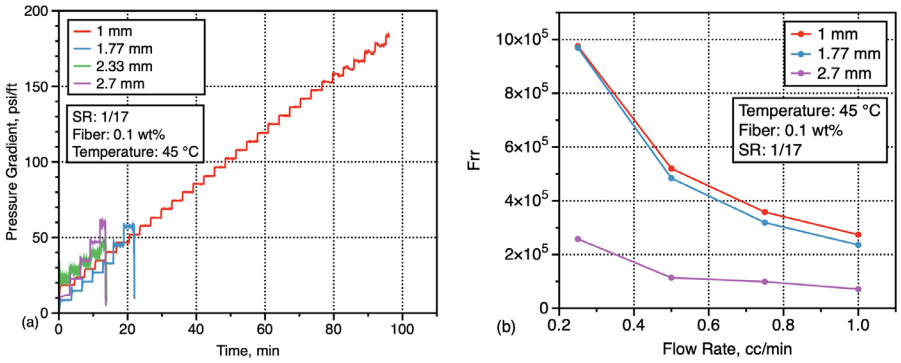

Fig. 16—Fracture width effect on water breakthrough (a) and F_{rr} (b).

Conclusions

We conducted a series of experiments using fracture models to investigate the effect of fiber on RPPG plugging performance. The following conclusions can be reached.

1. Fiber can accelerate the RPPG swelling rate but does not affect the time for RPPG to reach fully the swollen stage.
2. Fiber can significantly increase the recrosslinked RPPG bulk gel strength and plugging performance to fractures.

3. An optimized fiber concentration exists when it is added into RPPG. Too high fiber concentration results in the fiber entanglement problem, which can make the recrosslinked bulk gel inhomogeneous and allow the following injection of water to preferentially breakthrough its weak part.
4. A higher fiber concentration requires a longer time to stabilize injection pressure gradient, but fiber concentration does not affect the stable injection pressure gradient.
5. The plugging efficiency of fiber-assisted RPPG increases with the decrease of SR and fracture width.

Nomenclature

$\%$ = fiber content percentage is the weight percentage
k_{after} = permeability after gel treatment
k_{before} = permeability before gel treatment
$W_{RPPG\ particles}$ = weight of RPPG particles
$W_{feeding\ brine}$ = weight of feeding brine

References

Amir, Z., Said, I. M., and Jan, B. M. 2019. In Situ Organically Cross-Linked Polymer Gel for High-Temperature Reservoir Conformance Control: A Review. *Polym Adv Technol* **30** (1): 13–39. https://doi.org/10.1002/pat.4455.

Bai, B. and Sun, X. 2020. Development of Swelling-Rate Controllable Particle Gels to Control the Conformance of CO_2 Flooding. Paper presented at the SPE Improved Oil Recovery Conference, Virtual, 31 August–4 September. SPE-200339-MS. https://doi.org/10.2118/200339-MS.

Bai, B., Zhou, J., and Yin, M. 2015. A Comprehensive Review of Polyacrylamide Polymer Gels for Conformance Control. *Pet Expl Dev* **42** (4): 525–532. https://doi.org/10.1016/S1876-3804(15)30045-8.

Bai, B., Li, L., Liu, Y. et al. 2007a. Preformed Particle Gel for Conformance Control: Factors Affecting Its Properties and Applications. *SPE Res Eval & Eng* **10** (4): 415–422. SPE-89389-PA. https://doi.org/10.2118/89389-PA.

Bai, B., Liu, Y., Coste, J. P. et al. 2007b. Preformed Particle Gel for Conformance Control: Transport Mechanism Through Porous Media. *SPE Res Eval & Eng* **10** (2): 176–184. SPE-89468-PA. https://doi.org/10.2118/89468-PA.

He, X., Sinan, M., Kwak, H. et al. 2021. A Corrected Cubic Law for Single-Phase Laminar Flow through Rough-Walled Fractures. *Adv Water Res* **154**. https://doi.org/10.1016/j.advwatres.2021.103984.

Heidari, S., Ahmadi, M., Esmaeilzadeh, F. et al. 2019. Oil Recovery from Fractured Reservoirs Using in Situ and Preformed Particle Gels in Micromodel Structures. *J Petrol Explor Prod Technol* **9** (3): 2309–2317. https://doi.org/10.1007/s13202-019-0627-8.

Pu, J., Bai, B., Alhuraishawy, A. et al. 2019. A Recrosslinkable Preformed Particle Gel for Conformance Control in Heterogeneous Reservoirs Containing Linear-Flow Features. *SPE J.* **24** (4): 1714–1725. SPE-191697-PA. https://doi.org/10.2118/191697-PA.

Seright, R. S. 1997. Use of Preformed Gels for Conformance Control in Fractured Systems. *SPE Prod & Fac* **12** (1): 59–65. SPE-35351-PA. https://doi.org/10.2118/35351-PA.

Seright, R. S. 1999. Polymer Gel Dehydration During Extrusion Through Fractures. *SPE Prod & Fac* **14** (2): 110–116. SPE-56126-PA. https://doi.org/10.2118/56126-PA.

Seright, R. S. 2003. Washout of Cr(III)-Acetate-HPAM Gels from Fractures. Paper presented at the International Symposium on Oilfield Chemistry, Houston, Texas, USA, 5–7 February. SPE-80200-MS. https://doi.org/10.2118/80200-MS.

Seright, R. S., Lane, R. H., and Sydansk, R. D. 2001. A Strategy for Attacking Excess Water Production. Paper presented at the SPE Permian Basin Oil and Gas Recovery Conference, Midland, Texas, USA, 15–17 May. SPE-70067-MS. https://doi.org/10.2118/70067-MS.

Targac, G., Gallo, C., Smith, D. et al. 2020. Case History of Conformance Solutions for West Sak Wormhole/Void Space Conduit with a New Reassembling Pre-Formed Particle Gel RPPG. Paper presented at the SPE Annual Technical Conference and Exhibition, Virtual, 26–29 October. SPE-201302-MS. https://doi.org/10.2118/201302-MS.

Wang, Z., Bai, B., Sun, X. et al. 2019a. Effect of Multiple Factors on Preformed Particle Gel Placement, Dehydration, and Plugging Performance in Partially Open Fractures. *Fuel* **251**: 73–81. https://doi.org/10.1016/j.fuel.2019.04.027.

Wang, Z., Bai, B., Zhou, E. et al. 2019b. Experimental Evaluation of Oxidizing Breakers for a Polyacrylamide-Based Re-Crosslinkable Preformed Particle Gel. *Energy Fuels* **33** (6): 5001–5010. https://doi.org/10.1021/acs.energyfuels.9b00709.

Zhang, H. and Bai, B. 2011. Preformed-Particle-Gel Transport Through Open Fractures and Its Effect on Water Flow. *SPE J.* **16** (2): 388–400. SPE-129908-PA. https://doi.org/10.2118/129908-PA.

Zhao, S., Zhu, D., and Bai, B. 2021. Experimental Study of Degradable Preformed Particle Gel (DPPG) as Temporary Plugging Agent for Carbonate Reservoir Matrix Acidizing to Improve Oil Recovery. *J Pet Sci Eng* **205**. https://doi.org/10.1016/j.petrol.2021.108760.